

Flatness-based nonlinear control strategies for trajectory tracking of quadcopter systems

Thinh Nguyen^a, Ionela Prodan^a, Laurent Lefèvre^a

^a*Univ. Grenoble Alpes, LCIS, F-26902, Valence, France*

Abstract

This paper proposes several nonlinear control strategies for trajectory tracking of a quadcopter system based on the property of differential flatness. Its originality is twofold. Firstly, it provides a flat output for the quadcopter dynamics capable of creating full flat parametrization of the states and inputs. Moreover, B-splines characterizations of the flat output and their properties allow for optimal trajectory generation subject to way-point constraints. Secondly, several control strategies based on computed torque control and feedback linearization are presented and compared. The advantages of flatness within each control strategy are analyzed and detailed through extensive simulation results.

Keywords: Trajectory tracking; Differential flatness; B-splines parametrization; Feedback linearization; Quadcopter unmanned vehicle

1. Introduction

Recently, there has been an increasing interest in multiple research communities for the Unmanned Aerial Vehicles (UAVs) investigating on kinematics and dynamics, trajectory generation, guidance, navigation and control, especially
5 for quadcopters [1, 2, 3, 4, 5, 6]. The quadcopters seem to become popular only in the last decades but in fact, their concepts appeared more than a century ago. The first prototype, which was built in 1907 and named Brequet-Richet

Email addresses: ngoc-thinh.nguyen@lcis.grenoble-inp.fr (Thinh Nguyen),
ionela.prodan@lcis.grenoble-inp.fr (Ionela Prodan),
laurent.lefevre@lcis.grenoble-inp.fr (Laurent Lefèvre)

Gyrolane No.1, is reported to have lifted into flight [7]. Nowadays, quadcopters are being widely used in different domains and for many purposes such as re-
10 search platform [1, 8, 3, 4, 5, 6], military enforcement [9], commercial use [10]
as well as being in concept for medical emergency [11].

For the research area, quadcopters are challenging vehicles to control as they are not only strongly nonlinear and underactuated but also subject to many operating constraints. One feasible approach is to generate off-line a reference
15 path that allows tracking of specific objectives (i.e., passing through a priori given way-points, consumption minimization, state/input constraints satisfaction). Then, develop an effective tracking mechanism for the quadcopter to follow the reference at run-time [12]. As a result, generating a trajectory which respects the internal dynamics of the system and various external constraints,
20 becomes part of the problem.

A popular solution for trajectory generation is the use of flat output characterizations [13]. These allow implicitly to validate the dynamics and may (with some difficulty) take into account constraints. There is a number of works like [3, 14, 15, 16] which employ differential flatness within the trajectory track-
25 ing control design. However, these approaches are lacking in several essential directions:

- simplified dynamics (usually the yaw angle and/or the thrust are kept constant) are used to generate the trajectory and hence tracking errors may ensue;
- 30 • part of the available information provided by the trajectory is discarded at runtime (e.g., only position information is taken into account).

From the control point of view, there are various quadcopter control strategies like Lyapunov-based control [17], classical PID control [18, 19], LQR (Linear-quadratic regulator) control [8, 18], feedback linearization [3] or optimization-
35 based control [15]. Each of these approaches has some significant shortcomings:

- the control mechanism considers only altitude and attitude components and discards the rest of the state components [17]. As a remark, Lyapunov

function and corresponding stabilization controller [20, 17] may be difficult to find in other specific cases (e.g., controlling the position and direction angle of the quadcopter system);

- PID or LQR controllers (which are designed for a certain linearized model) are used to close the loop for the strongly non-linear dynamics of the quadcopter; this limits the performances of the scheme and requires for stay around the equilibrium point along which the linearization has been done [18, 19];
- even when nonlinear dynamics are taken into account, simplifications and approximations are made (e.g., constant yaw angle [21, 3], small angles [5], constant velocity [12]).

These simplifications for both trajectory generation and tracking mechanisms are apologized by the inherent complexity of the quadcopter dynamics but they raise two questions: *how can we make use of the full information provided by flatness? and, is it possible to control the quadcopter system considering its full behavior?*

To overcome the difficulties in processing the nonlinearities of a quadcopter system and all the above mentioned shortcomings, we propose in the rest of the paper several contributions which, to the best of our knowledge, are new to the state of the art:

- construct a flat trajectory which provides positions, angles, thrust and torques, considering the nonlinear quadcopter dynamics (throughout the paper we use B-splines characterizations of the flat output and their properties, which allow for optimal trajectory generation subject to way-point constraints [22]);
- delve into several control strategies based on the concept of feedback linearization which can control both orientation and position of the quadcopter system without any assumptions or simplifications on the system (as the assumptions of the nullified yaw angle [21, 3] or small angles [5]).

The remaining paper is organized as follows. Section 2 presents an in-depth view of the kinematics and dynamics modeling of a quadcopter system. Section 3 presents the flatness-based quadcopter characterization which fully takes
70 into account the system dynamics. Section 4 details some effective constructions for the rotation and attitude controllers of a quadcopter system based on feedback linearization. These constructions are further used to develop trajectory tracking control strategies making full use of the information provided by flatness. Extensive simulation results and comparisons between the proposed
75 control strategies are provided in Section 5 over a Crazyflie quadcopter system. Section 6 presents the conclusions and future work.

2. Quadcopter modelling

This section introduces the kinematics and the associated dynamics of the quadcopter using Newton-Euler formalism (more information can be found in
80 [3, 4]). The quadcopter will operate in two different coordinate systems: the *body reference frame* (BF) which is attached to the mass center of the quadcopter and the *inertial reference frame* (IF) which is fixed to the ground (East-North-Up coordinates). Upper-scripts B and I will be used to denote a variable measured in the BF and in the IF, respectively.

85 2.1. Kinematics

The angular position (or attitude) of the quadcopter is defined by the orientation of the BF with respect to the IF. In general, this relation is described through a 3D rotation matrix which is the product of the sequence of three successive rotations. For the quadcopter we apply the roll-pitch-yaw XYZ (ϕ, θ, ψ)

90 sequence whose rotation matrix is ¹(similar results can be found in [3, 5]):

$${}^I_B R = R_Z(\psi)R_Y(\theta)R_X(\phi) = \begin{bmatrix} c\theta c\psi & s\phi s\theta c\psi - c\phi s\psi & c\phi s\theta c\psi + s\phi s\psi \\ c\theta s\psi & s\phi s\theta s\psi + c\phi c\psi & c\phi s\theta s\psi - s\phi c\psi \\ -s\theta & s\phi c\theta & c\phi c\theta \end{bmatrix}, \quad (1)$$

The quadcopter has the angular velocity vector $\vec{\omega}$ pointing along the axis of rotation. We use the right hand rule to determine the direction of the rotation corresponding to the one of the angular velocity vector. Therefore, the angular velocity vector $\vec{\omega}$ looked from the BF ${}^B\vec{\omega} \triangleq [\omega_x \ \omega_y \ \omega_z]^\top$ ² can be expressed
 95 in term of the attitude as (the inverse relation can be found in [3, 5]):

$${}^B\vec{\omega} = \begin{bmatrix} 1 & 0 & -s\theta \\ 0 & c\phi & s\phi c\theta \\ 0 & -s\phi & c\phi c\theta \end{bmatrix} \begin{bmatrix} \dot{\phi} \\ \dot{\theta} \\ \dot{\psi} \end{bmatrix} = W\dot{\eta}, \quad (2)$$

where $\eta \triangleq [\phi \ \theta \ \psi]^\top$.

2.2. Dynamics

The quadcopter structure and the BF are presented in Figure 1 including the corresponding angular velocities ω_i , torques τ_i and forces f_i created by the
 100 four rotors, with $i = 1, \dots, 4$.

From the aerodynamic effects viewpoint, we can express the torque τ_i about the z_B axis³ and the forces f_i along z_B direction for the i^{th} rotor as:

$$\tau_i = (-1)^i b\omega_i^2 + I_M \dot{\omega}_i \approx (-1)^i b\omega_i^2, \quad (3)$$

$$f_i = K_T \omega_i^2, \quad (4)$$

where $i = 1, \dots, 4$, I_M is the moment of inertia of the motor about the rotational axis, b and K_T are assumed known aerodynamic constants.

¹Note that, in order to write in a more compact way we have used in this paper ' s ', ' c ' and ' t ' to denote the $\sin(\cdot)$, $\cos(\cdot)$ and $\tan(\cdot)$ functions, respectively.

²Note that the angular velocity ${}^B\vec{\omega}$ is physically measured by the gyroscope.

³ $(-1)^i b\omega_i^2$ term is positive if the i^{th} propeller is spinning clockwise and negative if it is spinning counterclockwise

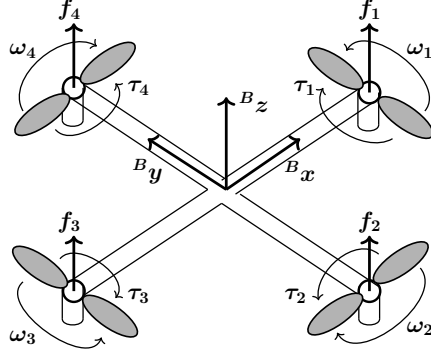


Figure 1: Quadcopter system.

Furthermore, the total thrust force and torques acting on the quadcopter have the magnitudes as:

$$T = \sum_{i=1}^4 f_i = K_T \sum_{i=1}^4 \omega_i^2, \quad (5)$$

$$\tau_\phi = Lf_4 - Lf_2 = LK_T (\omega_4^2 - \omega_2^2), \quad (6)$$

$$\tau_\theta = Lf_3 - Lf_1 = LK_T (\omega_3^2 - \omega_1^2), \quad (7)$$

$$\tau_\psi = \sum_{i=1}^4 \tau_i = b (-\omega_1^2 + \omega_2^2 - \omega_3^2 + \omega_4^2), \quad (8)$$

where L is the distance from the center of the quadcopter to any propellers. Note that, expressing in BF, the thrust force is defined as $\vec{B}T \triangleq [0 \ 0 \ T]^T$ and $\vec{\tau}_\phi, \vec{\tau}_\theta, \vec{\tau}_\psi$ have corresponding directions along the three axes of BF.

2.2.1. Translation equation

105

In the IF, assuming that the centrifugal force is nullified, hence, only gravitational force, $m\vec{g}$, thrust force, $\vec{B}T$ and external perturbation force (most commonly, friction), \vec{F}_D are contributing to the acceleration of the quadcopter:

$$m\ddot{\xi} = m\vec{g} + ({}^I_B R)\vec{B}T + \vec{F}_D, \quad (9)$$

where $\xi \triangleq [x \ y \ z]^\top$ represents the quadcopter position, the thrust force $\overrightarrow{B}T$ has
 110 the magnitude defined in equation (5) and the perturbation force \overrightarrow{F}_D will be
 detailed later in Section 2.2.3.

2.2.2. Rotation equation

While it looks convenient to have the linear equations of motion in the IF, the
 115 rotational equations are more useful in the BF. We assume that the quadcopter
 has a symmetrical construction, hence, the inertial tensor ${}^B I$ is a diagonal ma-
 trix:

$${}^B I = \text{diag}\{I_{xx}, I_{yy}, I_{zz}\}. \quad (10)$$

In vector form, the Newton-Euler rotational equation for the quadcopter in BF
 taking into account the gyroscopic force is defined as:

$${}^B I \dot{\overrightarrow{\omega}} + {}^B \overrightarrow{\omega} \times ({}^B I \overrightarrow{\omega}) = \tau_\eta, \quad (11)$$

120 where ‘ \times ’ denotes the cross-product of two vectors and $\tau_\eta \triangleq [\tau_\phi \ \tau_\theta \ \tau_\psi]^\top$ gathers
 the roll, pitch and yaw torques which have been detailed in equations (6)–(8).

2.2.3. Perturbation force

In order to make the model more realistic and able to take into account air
 125 disturbances, we model the external perturbation force triggered by the quad-
 copter motion and the external wind. Based on the definition of friction force
 found in [23], the vector of global friction force is given by:

$$\overrightarrow{F}_D = \frac{1}{2} C_D \rho |\overrightarrow{V}_r| A \overrightarrow{V}_r, \quad (12)$$

where ρ is the surrounding fluid density, C_D is the drag coefficient, $\overrightarrow{V}_r = \overrightarrow{w} - \dot{\xi}$
 is the vector of relative motion between the wind speed \overrightarrow{w} and the quadcopter
 130 velocity $\dot{\xi}$. In equation (12), the projected area A is calculated by the following
 relation:

$$A = A_x \left| \frac{\overrightarrow{i}_{x_B} \overrightarrow{V}_r}{|\overrightarrow{V}_r|} \right| + A_y \left| \frac{\overrightarrow{i}_{y_B} \overrightarrow{V}_r}{|\overrightarrow{V}_r|} \right| + A_z \left| \frac{\overrightarrow{i}_{z_B} \overrightarrow{V}_r}{|\overrightarrow{V}_r|} \right|, \quad (13)$$

where A_x, A_y, A_z , which depend on the designed structure of the quadcopter, describe the projected areas into YZ, XZ, and XY planes of the BF. In equation (13), $\vec{I}_{x_B}, \vec{I}_{y_B}$ and \vec{I}_{z_B} represent the three column vectors of the rotation matrix ${}^I_B R$ given in (1).

3. Flat characterizations

This section introduces first some basic definitions and notions on differential flatness and B-splines parametrization [22, 12]. Next, a novel flatness-based characterization which fully takes into account the dynamics of the quadcopter system is described.

3.1. Basic definitions

Differential flatness represents a generalization to nonlinear systems of the structural properties of the linear systems, which exhibit a state representation obtained via derivatives of the input and output signals.

Consider a general system:

$$\dot{\mathbf{x}}(t) = f(\mathbf{x}(t), \mathbf{u}(t)), \quad (14)$$

where $x(t) \in \mathbb{R}^n$ is the state vector and $u(t) \in \mathbb{R}^m$ is the input vector. The nonlinear system written in general form as in equation 14 is called differentially flat if there exists a flat output $\mathbf{z}(t) \in \mathbb{R}^m$:

$$\mathbf{z}(t) = \Upsilon(\mathbf{x}(t), \mathbf{u}(t), \dot{\mathbf{u}}(t), \dots, \mathbf{u}^{(q)}(t)), \quad (15)$$

such that the states and inputs can be algebraically expressed in terms of $\mathbf{z}(t)$ and a finite number of its higher-order derivatives:

$$\mathbf{x}(t) = \Upsilon_1(\mathbf{z}(t), \dot{\mathbf{z}}(t), \dots, \mathbf{z}^{(q)}(t)), \quad (16a)$$

$$\mathbf{u}(t) = \Upsilon_2(\mathbf{z}(t), \dot{\mathbf{z}}(t), \dots, \mathbf{z}^{(q+1)}(t)). \quad (16b)$$

Remark 1. Note that the flatness and controlability properties of a system are directly related. It is demonstrated that a linear system is flat if and only if it is controllable [24][13]. Furthermore, for any system admitting a flatness-based representation, the number of flat outputs equals the number of inputs. \square

An essential aspect of construction (15)–(16) is that it reduces the problem of trajectory generation to finding an adequate flat output (15). This means choosing $\mathbf{z}(t)$ such that, via mappings Υ_1, Υ_2 , various constraints on states and inputs (16) are verified. Since the flat output is not straightforward to compute under these restrictions, usually a projection across a finite basis of smooth functions $\Lambda^i(t)$ is considered:

$$\mathbf{z}(t) = \sum_{i=1}^n \alpha_i \Lambda^i(t), \quad \alpha_i \in \mathbb{R}. \quad (17)$$

Parameter n in equation (17) depends on the number of constraints imposed onto the system [25].

There are multiple choices for the basis functions $\Lambda^i(t)$. Among these, *B-spline* basis functions are well-suited to flatness parametrization due to their ease of enforcing continuity and because their degree depends only up to which derivative is needed to ensure continuity [26, 27].

A B-spline of order d is characterized by a *knot-vector* [28]:

$$\mathbb{T} = \{\tau_0, \tau_1 \dots \tau_m\}, \quad (18)$$

of non-decreasing time instants ($\tau_0 \leq \tau_1 \leq \dots \leq \tau_m$) which parametrizes the associated basis functions $B_{i,d}(t)$:

$$B_{i,1}(t) = \begin{cases} 1, & \text{for } \tau_i \leq t < \tau_{i+1} \\ 0 & \text{otherwise} \end{cases}, \quad (19a)$$

$$B_{i,d}(t) = \frac{t - \tau_i}{\tau_{i+d-1} - \tau_i} B_{i,d-1}(t) + \frac{\tau_{i+d} - t}{\tau_{i+d} - \tau_{i+1}} B_{i+1,d-1}(t), \quad (19b)$$

for $d > 1$ and $i = 0, 1 \dots n = m - d$. Considering a collection of *control points*

$$\mathbb{P} = \{p_0, p_1 \dots p_n\}, \quad (20)$$

we define a *B-spline curve* as a linear combination of the control points (20) and the B-spline functions (19a)–(19b):

$$\mathbf{z}(t) = \sum_{i=0}^n B_{i,d}(t) p_i = \mathbf{P} \mathbf{B}_d(t), \quad (21)$$

where $\mathbf{P} = [p_0 \dots p_n]$ and $\mathbf{B}_d(t) = [B_{0,d}(t) \dots B_{n,d}(t)]^\top$. This construction
 170 yields several interesting properties which are enumerated in [22].

Let us consider now a collection of $N + 1$ way-points and the time stamps associated to them:

$$\mathbb{W} = \{w_k\} \text{ and } \mathbb{T}_{\mathbb{W}} = \{t_k\}, \quad (22)$$

for any $k = 0 \dots N$. The goal is to construct a flat trajectory which passes through each way-point w_k at the time instant t_k , i.e., find a flat output $\mathbf{z}(t)$
 175 such that

$$\mathbf{x}(t_k) = \Upsilon_1(\mathbf{z}(t_k), \dots \mathbf{z}^{(q)}(t_k)) = w_k, \forall k = 0 \dots N. \quad (23)$$

Within the B-spline framework (21) we provide a vector of control points (20) and its associated knot-vector (18) such that condition (23) is verified:

$$\Upsilon_1(\mathbf{B}_d(t_k), \mathbf{P}) = w_k, \forall k = 0 \dots N. \quad (24)$$

Let us assume that the knot-vector is fixed ($\tau_0 = t_0$, $\tau_{n+d} = t_N$ and the intermediary points τ_d, \dots, τ_n are equally distributed along these extremes). Then,
 180 we can write an optimization problem with control points p_i as decision variables⁴ whose goal is to minimize a state and/or input integral cost $\Xi(\mathbf{x}(t), \mathbf{u}(t))$ along the time interval $[t_0, t_N]$:

$$\mathbf{P} = \arg \min_{\mathbf{P}} \int_{t_0}^{t_N} \|\tilde{\Xi}(\mathbf{B}_d(t), \mathbf{P})\|_Q dt, \quad (25)$$

s.t. constraints (24) are verified,

with Q a positive symmetric matrix. The cost in (25) can impose any penalization we deem necessary (length of the trajectory, input variation/magnitude,
 185 energy minimization and the like).

3.2. Flatness-based system representation

By replacing the rotation matrix (1) in the translation equation (9) and disregarding the perturbation force as well as replacing the inertia tensor (10)

⁴Since the B-spline curve is clamped (see for more details [22]) it means that the extreme control points are already fixed: $\Upsilon_1(p_0 = \mathbf{z}(t_0)) = w_0$ and $\Upsilon_1(p_n = \mathbf{z}(t_N)) = w_N$.

in the rotation equation (11), we obtain the matrix form of the quadcopter dynamics:

$$\begin{bmatrix} \ddot{x} \\ \ddot{y} \\ \ddot{z} \end{bmatrix} = \begin{bmatrix} 0 \\ 0 \\ -g \end{bmatrix} + \frac{1}{m} \begin{bmatrix} c\phi s\theta c\psi + s\phi s\psi \\ c\phi s\theta s\psi - s\phi c\psi \\ c\phi c\theta \end{bmatrix} T, \quad (26)$$

$$\begin{bmatrix} \dot{\omega}_x \\ \dot{\omega}_y \\ \dot{\omega}_z \end{bmatrix} = \begin{bmatrix} (I_{yy} - I_{zz})I_{xx}^{-1}\omega_y\omega_z \\ (I_{zz} - I_{xx})I_{yy}^{-1}\omega_z\omega_x \\ (I_{xx} - I_{yy})I_{zz}^{-1}\omega_x\omega_y \end{bmatrix} + \begin{bmatrix} I_{xx}^{-1}\tau_\phi \\ I_{yy}^{-1}\tau_\theta \\ I_{zz}^{-1}\tau_\psi \end{bmatrix}. \quad (27)$$

Considering the nonlinear dynamics (26) we derive the following flat output vector $\mathbf{z} \in \mathbb{R}^4$ whose dimension equals to the number of inputs $[T \ \tau_\phi \ \tau_\theta \ \tau_\psi]^\top$:

$$\mathbf{z} = [z_1 \ z_2 \ z_3 \ z_4]^\top = \left[x \ y \ z \ \tan\left(\frac{\psi}{2}\right) \right]^\top, \quad (28)$$

which will be used to describe the remaining states and inputs (roll, pitch, yaw, thrust and the like):

$$\phi = \arcsin\left(\frac{2z_4\ddot{z}_1 - (1 - z_4^2)\ddot{z}_2}{(1 + z_4^2)\sqrt{\ddot{z}_1^2 + \ddot{z}_2^2 + (\ddot{z}_3 + g)^2}}\right), \quad (29)$$

$$\theta = \arctan\left(\frac{(1 - z_4^2)\ddot{z}_1 + 2z_4\ddot{z}_2}{(1 + z_4^2)(\ddot{z}_3 + g)}\right), \quad (30)$$

$$\psi = 2 \arctan(z_4), \quad (31)$$

$$T = m\sqrt{\ddot{z}_1^2 + \ddot{z}_2^2 + (\ddot{z}_3 + g)^2}. \quad (32)$$

Gathering the angular velocity detailed in (2) into the rotation equation (11),

190 we obtain the torques described in term of the angular positions:

$$\tau_\eta = {}^B I \left(W\ddot{\eta} + \dot{W}\dot{\eta} \right) + (W\dot{\eta}) \times ({}^B I W\dot{\eta}), \quad (33)$$

which can be easily interpreted in the flat output space by introducing (29)–(31) and which we do not show here due to their convoluted representation.

With respect to the notation in (16), mapping $\Upsilon_1(\cdot)$ comes from (28)–(31) (with a derivation degree $q = 3$) and mapping $\Upsilon_2(\cdot)$ from (32) and the expansion of (33) (with a derivation degree $q + 1 = 4$). For further use we denote

195

$\Upsilon_\xi(\cdot), \Upsilon_\eta(\cdot), \Upsilon_T(\cdot), \Upsilon_{\tau_\eta}(\cdot)$ the mappings which map \mathbf{z} into the corresponding variable (e.g., $\xi = \Upsilon_\xi(\mathbf{z})$).

Remark 2. Note that, there exist necessary and sufficient conditions for differential flatness as well as the "sequential"⁵ procedure used to test if the system is flat [24]. Some insights on the procedure are summarized here.

Considering the general system (14) with f smooth, under several specific conditions described in [24], there exists an underdetermined implicit system F with dimension of $n - m$ satisfying [24]:

$$\text{rank} \left(\frac{\partial f}{\partial \mathbf{u}} \right) = m \Leftrightarrow \exists F(\mathbf{x}, \dot{\mathbf{x}}) = 0, \text{rank} \left(\frac{\partial F}{\partial \dot{\mathbf{x}}} \right) = n - m, \quad (34)$$

where n is the number of states and m is the number of inputs.

Equation (34) shows that $n-m$ implicit functions F suffice to express the dynamics of f . Consequently, we may find m variables which can be used to express all the remaining $n - m$ variables. These m variables can be taken as the flat outputs used to describe the rest of the states and the inputs. Similarly, we can follow the sequential procedures provided in [24] to feasibly obtain the flat output representation.

For our particular case (26),(27), the two important implicit functions are:

$$s\phi\sqrt{\ddot{x}^2 + \ddot{y}^2 + (\ddot{z} + g)^2} - s\psi\ddot{x} + c\psi\ddot{y} = 0, \quad (35a)$$

$$t\theta(\ddot{z} + g) - c\psi\ddot{x} - s\psi\ddot{y} = 0. \quad (35b)$$

One can easily describe ϕ, θ in terms of the four other states. As a result, the conventional flat output is proposed as $\mathbf{z} = [z_1 \ z_2 \ z_3 \ z_4]^\top = [x \ y \ z \ \psi]^\top$ which has been researched before [29, 21, 3]. We found that the 'naive' approach of taking $z_4 = \psi$ leads to extremely convoluted calculations, therefore, we introduce a new formulation in (28). \square

Remark 3. Other remarks can be made over the simplified version of flat representation usually employed in the state of the art [29, 21, 3]. Assuming that

⁵There is no guarantee that this procedure finishes in a finite number of steps [24].

yaw angle equals to zero, the formulation (29),(30) simplifies to:

$$\phi = \arcsin \left(\frac{-\ddot{z}_2}{\sqrt{\dot{z}_1^2 + \dot{z}_2^2 + (\dot{z}_3 + g)^2}} \right), \quad (36a)$$

$$\theta = \arctan \left(\frac{\dot{z}_1}{\dot{z}_3 + g} \right). \quad (36b)$$

The problem is that while tracking this trajectory the real dynamics will actually vary the yaw angle (a possible solution not followed here is to track $\psi = 0$ at the runtime). We do not follow these assumptions in the present paper since we want to exploit all the degrees of freedom, thus fully taking into account the nonlinear system dynamics (including the yaw angle). \square

Solving (25) over a B-spline parametrization as in Section 3.1 with the flat representation from (28)–(33) we have the general mapping:

$$\bar{\xi} = \Upsilon_{\xi}(\bar{\mathbf{z}}), \quad (37a)$$

$$\bar{\eta} = \Upsilon_{\eta}(\bar{\mathbf{z}}), \quad (37b)$$

$$\bar{T} = \Upsilon_T(\bar{\mathbf{z}}), \quad (37c)$$

$$\bar{\tau} = \Upsilon_{\tau}(\bar{\mathbf{z}}), \quad (37d)$$

where the flat output $\bar{\mathbf{z}}$, the flat states $\bar{\xi}, \bar{\eta}$ and the flat inputs $\bar{T}, \bar{\tau}$ are given by (28)–(33).

4. Control design for trajectory tracking

This section introduces first the general control strategy usually employed in the literature for a quadcopter system. Next, we propose two control design strategies based on the concept of feedback linearization and facilitated by the flatness construction detailed in Section 3.2. These first two strategies built for two different missions, control the attitude and the torques of the quadcopter, pave the way for additional control strategies which make more use of the information provided by the a priori generated flat trajectory, i.e., positions, angles, accelerations, thrust force. The idea behind the next three strategies is to use

the attitude and torque controllers combined with appropriate input references obtained from the flatness procedure introduced in Section 3.

235 4.1. General control scheme

A typical control scheme for quadcopters (and UAV systems in general) is depicted in Figure 2. The preferred approach is to consider two control layers, thus

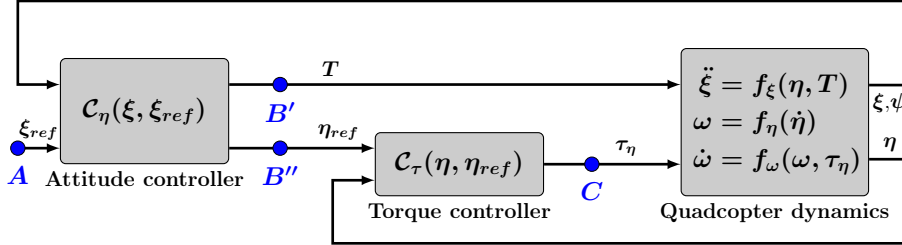


Figure 2: Control scheme for a quadcopter system.

exploiting the decoupling between the translational and rotational dynamics of the quadcopter. At the higher level, an *attitude controller* $C_\eta(\xi, \xi_{ref})$ compares an externally given reference position ξ_{ref} with the real position ξ and provides
 240 an attitude reference η_{ref} and thrust T . The latter is sent directly to the quadcopter and the former to the lower level *torque controller* $C_\tau(\eta, \eta_{ref})$ which compares it with the real angles η in order to provide the angle torques τ_η .

As also underlined in the control schema of Figure 2, the attitude controller
 245 provides attitude and thrust references. Usually this allows for simple movements like straight line tracking, circular movement around a fixed center, hovering at a fixed height and so forth. The torque controller provides the torques τ_η which enforce the quadcopter angular positions η to track their references η_{ref} . Standard control design methods for these two controllers can be found
 250 in [3, 5]. In these studies, they used the simplified model with zero yaw angle to obtain the attitude controller and classical PID regulator inside the torque controller. As mentioned before in Section 2, the quadcopter rotation dynamics are nonlinear system and are not suitable for linear PID controller. In what follows, we provide effective constructions for the torque and attitude controllers

255 based on feedback linearization which take into account the quadcopter dynam-
ics. These will be introduced in the forthcoming control design strategies via
flatness for trajectory tracking.

4.2. Torque controller

The proposed torque controller design builds upon the computed torque con-
260 trol concept which is a special application of feedback linearization of nonlinear
systems (basic notions and details on feedback linearization and, in particular,
computed torque control can be found in [30], [20]). It has gained popularity
in modern system theory by providing excellent tracking performance through
nonlinear compensations (assuming a precise dynamic model is available [31]).

265 Consider the reformulation of the rotational dynamics (33) as:

$$M(\eta)\ddot{\eta} + V(\eta, \dot{\eta}) = \tau_\eta, \quad (38)$$

with mappings $M(\eta)$, $V(\eta, \dot{\eta})$ of appropriate content, i.e, $M(\eta) = {}^B IW$ and
 $V(\eta, \dot{\eta}) = {}^B I\dot{W}\dot{\eta} + (W\dot{\eta}) \times ({}^B IW\dot{\eta})$.

By using the partitioned controller scheme introduced in [30], we take the
control law for angle torques as:

$$\tau_\eta = \alpha\tau' + \beta, \quad (39)$$

where α, β named model-based portion and τ' named servo portion are taken
as:

$$\alpha = M(\eta), \quad (40a)$$

$$\beta = V(\eta, \dot{\eta}), \quad (40b)$$

$$\tau' = \ddot{\eta}_{ref} + K_d\dot{\epsilon}_\eta + K_p\epsilon_\eta + K_i \int \epsilon_\eta dt, \quad (40c)$$

270 with $\epsilon_\eta = \eta_{ref} - \eta$. Introducing (39) into (38) leads to a linear error dynamics:

$$\ddot{\epsilon}_\eta + K_{d\eta}\dot{\epsilon}_\eta + K_{p\eta}\epsilon_\eta + K_{i\eta} \int \epsilon_\eta dt = 0. \quad (41)$$

Note that suitable parameters $K_{p\eta}$, $K_{d\eta}$, $K_{i\eta}$ (diagonal matrices from \mathbb{R}^3) need
to be chosen in (41) so that the system is stable. To this end the following
proposition is introduced.

Proposition 1. Consider a third order linear dynamic system with the bounded
 275 and continuous input U (e.g., perturbation triggered by a bounded and continuous
 wind gust) and the output E which is the scalar error between specific state
 and its reference:

$$\ddot{E} + K_d \dot{E} + K_p E + K_i \int E dt = U. \quad (42)$$

By choosing the scalar parameters K_p, K_d, K_i satisfying the conditions:

$$\begin{cases} K_p, K_d, K_i > 0 \\ K_p K_d > K_i \end{cases}, \quad (43)$$

the system (42) is uniformly asymptotically stable.

280 *Proof.* Gathering $k(t) = \int_0^t E(\tau) d\tau \Leftrightarrow E = \dot{k}$ into (42), we arrive to the new
 system in terms of $k(t)$:

$$k^{(3)} + K_d \ddot{k} + K_p \dot{k} + K_i k = U. \quad (44)$$

Applying the Laplace transform of $K(s) = \mathcal{L}(k(t))$ and $U(s) = \mathcal{L}(U(t))$ for (44),
 we get:

$$\begin{aligned} s^3 K(s) + K_d s^2 K(s) + K_p s K(s) + K_i K(s) &= U(s) \\ \Rightarrow \frac{K(s)}{U(s)} &= \frac{1}{s^3 + K_d s^2 + K_p s + K_i}. \end{aligned} \quad (45)$$

This linear time-invariant system (44) is BIBO stable, or in other words, the
 characteristic equation has all its roots with negative real parts if and only if
 parameters K_p, K_d, K_i satisfying condition (43) which is the Routh–Hurwitz
 285 criterion.

With bounded input U , the system results in bounded output $k(t)$ over the
 time interval $[t_0, \infty)$:

$$\|k(t)\| \leq C \quad \forall t \in [t_0, \infty), \quad C \in \mathcal{R} \quad (46)$$

$$\Rightarrow \left\| \int_0^t E(\tau) d\tau \right\| \leq C \quad \forall t \in [t_0, \infty), \quad C \in \mathcal{R}. \quad (47)$$

Next, we use the Barbalat's lemma [20] which states that a continuous function
 $f(t)$ satisfying $\lim_{t \rightarrow \infty} f(t) = \alpha$, $\alpha < \infty$, its continuous derivative $f'(t)$ satisfies

$\lim_{t \rightarrow \infty} f'(t) = 0$. Consequently, mapping $f(t), f'(t)$ to appropriate contents, e.g., $\int_0^t E(\tau) d\tau$ and $E(t)$ respectively, we already obtained the condition 47 and since $U(t)$ is continuous, it leads to the continuous $E(t)$. As the result, we come to the conclusion $\lim_{t \rightarrow \infty} E(t) = 0$. Thus completing the proof. \square

4.3. Attitude controller

In general, the attitude controller provides the thrust force T and the angle references η_{ref} which are necessary for the quadcopter to follow the position references ξ_{ref} . The proposed attitude controller design is also based on the concept of feedback linearization of nonlinear systems which will drive the translation dynamics to error dynamics similar with those in (41).

Considering the roll, pitch, yaw angles and input thrust T in terms of the flat output described in equations (29)–(32), they can be particularly expressed as $\phi = \Gamma_\phi(\ddot{z}_1, \ddot{z}_2, \ddot{z}_3, z_4)$, $\theta = \Gamma_\theta(\ddot{z}_1, \ddot{z}_2, \ddot{z}_3, z_4)$, $\psi = \Upsilon_\psi(z_4)$ and $T = \Gamma_T(\ddot{z}_1, \ddot{z}_2, \ddot{z}_3)$. We provide the reference to be followed (the output of the attitude controller from the scheme in Figure 2) as:

$$\phi_{ref} = \Gamma_\phi(\ddot{z}_1^*, \ddot{z}_2^*, \ddot{z}_3^*, z_4), \quad (48a)$$

$$\theta_{ref} = \Gamma_\theta(\ddot{z}_1^*, \ddot{z}_2^*, \ddot{z}_3^*, z_4), \quad (48b)$$

$$\psi_{ref} = \Upsilon_\psi(z_4), \quad (48c)$$

$$T = \Gamma_T(\ddot{z}_1^*, \ddot{z}_2^*, \ddot{z}_3^*), \quad (48d)$$

where the corrective term $\xi^* \triangleq [z_1^* \ z_2^* \ z_3^*]^\top$ is given as:

$$\xi^* = \xi_{ref} + K_{d\xi} \int \epsilon_\xi dt + K_{p\xi} \int \int \epsilon_\xi dt + K_{i\xi} \int \int \int \epsilon_\xi dt, \quad (49)$$

with $\epsilon_\xi = \xi_{ref} - \xi$ and $K_{p\xi}, K_{d\xi}, K_{i\xi}$ are diagonal matrices from \mathbb{R}^3 .

300

Taking into account the external perturbation force, gathering equations (48) into the translation equation (9) leads to the following relation:

$$\ddot{\xi} - \frac{\overrightarrow{F_D}}{m} = \ddot{\xi}_{ref} + K_{p\xi} \epsilon_\xi + K_{d\xi} \dot{\epsilon}_\xi + K_{i\xi} \int \epsilon_\xi dt, \quad (50)$$

which results in the error dynamics:

$$\ddot{\epsilon}_\xi + K_{p\xi}\epsilon_\xi + K_{d\xi}\dot{\epsilon}_\xi + K_{i\xi} \int \epsilon_\xi dt = -\frac{\vec{F}_D}{m}, \quad (51)$$

similarly to Proposition 1.

305 In what follows, the attitude and torque controllers will prove useful for additional strategies which allow feedback control via planned flat trajectory.

4.4. Flat angle tracking

Starting from the lower level and using only the torque controller introduced in Section 4.2, it is possible to control the quadcopter by providing directly
310 the input components T and η_{ref} obtained by the flatness-based trajectory generation (insertion at points B' and B'' in Figure 2):

$$T = \bar{T}, \quad \eta_{ref} = \bar{\eta}. \quad (52)$$

Then, the torque controller gives the angle torques τ_η as detailed in Section 4.2. According to Proposition 1, the quadcopter rotating system will be asymptotically stable.

315 Applying this strategy, the angle tracking leads actually to the position tracking in the predicted case ⁶. Note that from a practical viewpoint, this strategy is realistic for small-scale quadcopters, (e.g., flycam, radio controller quadcopter) since the angle feedback can be approximately obtained by available sensors such as gyroscope, accelerometer and geomagnetic field sensor, while the
320 position feedback is difficult to retrieve. It is worth underlining that this open-loop functioning for position is sensitive to disturbances and other sources of error. To counteract this limitation, in the next section we will introduce a position feedback loop.

⁶The predicted case is the combination of reference trajectory coming with wind information used in the flatness procedure.

4.5. Flat position tracking

325 This controller which is based on the attitude controller presented in Section 4.3, compares the reference $\bar{\xi}$ and real position ξ and provides the thrust force T and angle torques τ_η . The general idea is well illustrated in Figure 2:

- The trajectory generation provides the references $\bar{\xi}$ and \bar{z}_4 (insertion at point A) as in (37).
 - 330 - The attitude controller provides thrust force (insertion at point B') and necessary angles $\eta_{ref} \triangleq [\phi_{ref} \ \theta_{ref} \ \psi_{ref}]^\top$ as introduced in equation (48) but in terms of \bar{z}_4 in stead of z_4 .
 - The angle torques τ_η are calculated based on the rotation equation (33) in terms of η_{ref} , then, sent to the quadcopter system (insertion at point C).
- 335

This controller, as we will also validate through simulations, achieves the good results for position tracking. Note that, the quadcopter position can be straightforward to be observed by using GPS (Global Positioning System). One solution is through the use of the technique called *differential GPS* or *dual*
340 *frequency GPS* which gives a resolution of 1 m, if a second static receiver at a known exact position is employed [20]. However, the open-loop functioning for angle of this strategy generates various errors of yaw angle ψ .

Next, a combination of the two above procedures is discussed.

4.6. Combined flat angle and position tracking

345 Considering the two previous strategies, we recognized the necessity of both position and angle feedback. Hence, this controller design follows the two-layer classical control strategy described in 4.1. More precisely, at the upper level we use the attitude controller detailed in Section 4.3 which compares the position reference $\bar{\xi}$ and the real position ξ to provide the thrust T (48d) and the reference angles $\eta_{ref} = [\phi_{ref} \ \theta_{ref} \ \psi_{ref}]^\top$ (48a-48c). The angles are sent to
350 the lower level which is the torque controller detailed in Section 4.2. The torque

controller provides the angle torques τ_η to the quadcopter system. Note that, the quadcopter position feedback is necessary for the attitude controller and the orientation for the torque controller. Assuming we have at our disposal all of the ideal necessary sensors, this strategy provides the best trajectory tracking results which will be demonstrated and compared in the next section.

5. Simulation results and comparison

In this section, we first present simulation results of our control strategies introduced in section 4. Then, various comparisons of our contributions with other flatness-based control approaches [15, 21, 3, 32] are provided.

5.1. Simulation results

This section presents extensive simulation results for a Crazyflie 2.0 quadcopter [33] characterized by the following parameters:

- each of the four propellers has bounds on the (load-free) rotating speed $|\omega_i| \leq 58800$ [rpm] and angular acceleration $|\Delta\omega_i| \leq 1000$ [rad/s²];
- $g = 9.81$ [m/s²], $m = 0.5$ [kg], $L = 0.225$ [m], $K_T = 2.98 \times 10^{-6}$ [kgm], $b = 1.14 \times 10^{-7}$ [kgm²], $I_{xx} = I_{yy} = 4.856 \times 10^{-3}$ [kgm²], $I_{zz} = 8.801 \times 10^{-3}$ [kgm²].

The simulation scenarios consider a collection of way-points $\mathbb{W} = \{[0 \ 0 \ 5]^\top, [0.4 \ 0.9 \ 6]^\top, [1.4 \ 1.2 \ 6.5]^\top, [2 \ 0.8 \ 5.7]^\top, [1.5 \ -0.5 \ 5]^\top\}$ with the associated time instants $\{0, 3, 5.5, 7, 10\}$ second.

We implement the optimization problem (25) by choosing to minimize the total trajectory length and to pass through the a priori given way-points in a total time $T = 10$ s. We consider B-spline basis functions of degree $d = 6$ and a collection of 12 control points as in (20) for the flat output parametrization. The resulting trajectory, position, angles⁷, thrust and torques are depicted in

⁷We used a standard polynomial function $z_4(t)$ for $\psi(t)$ to smoothly increase from 0 to 10 degrees in 10s.

Figure 3 and Figure 4.

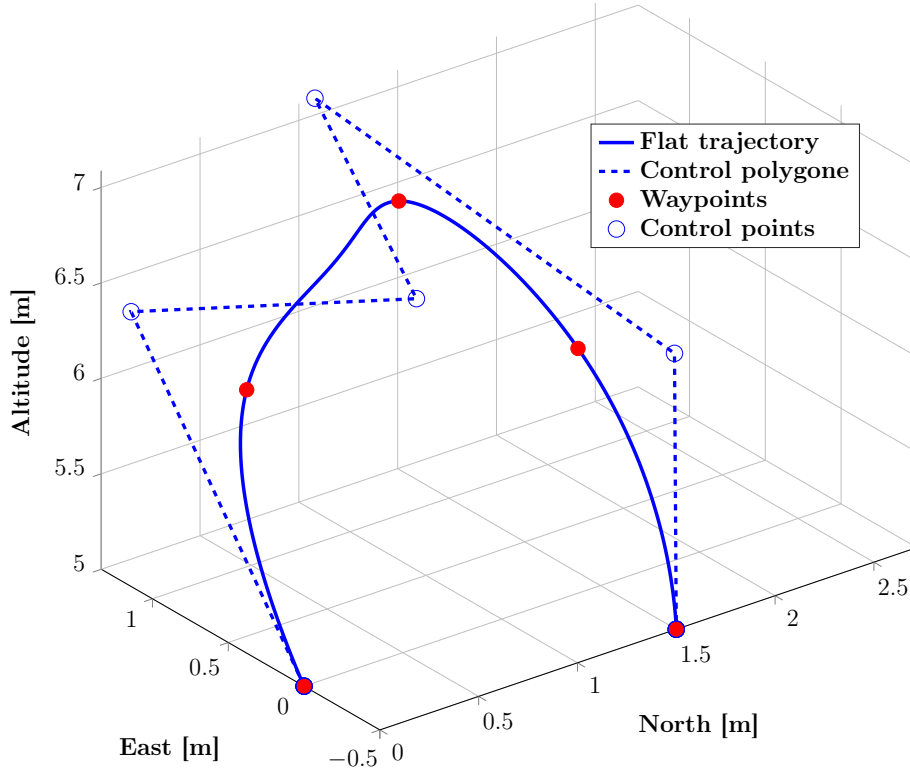
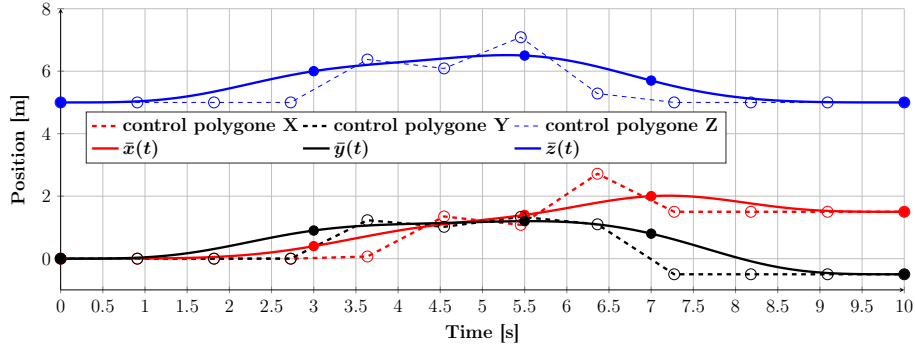
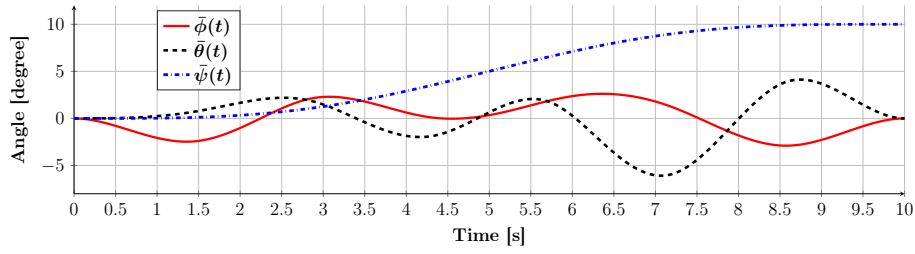


Figure 3: B-spline parametrized flat trajectory with the associated control points and passing through way-points.

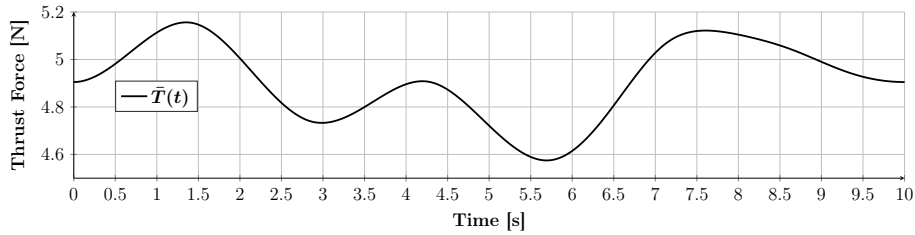
In what follows we consider the various control strategies discussed in Section 4 and apply them for the reference trajectory generated earlier. For each of these approaches we consider two cases of no wind and wind profile with a maximum speed up to 25 [km/h] (the values are taken from www.meteoblue.com over the year 2015 in Rhône Alpes region, France). The control algorithms implementation are done using Yalmip [34], MPT Toolboxes [35] in Matlab/Simulink 2015a over a horizon of $T = 10$ sec with a fixed sampled time of 0.01 sec. The tuning parameters K_p , K_i , K_d of each controller are delineated in Table 1.



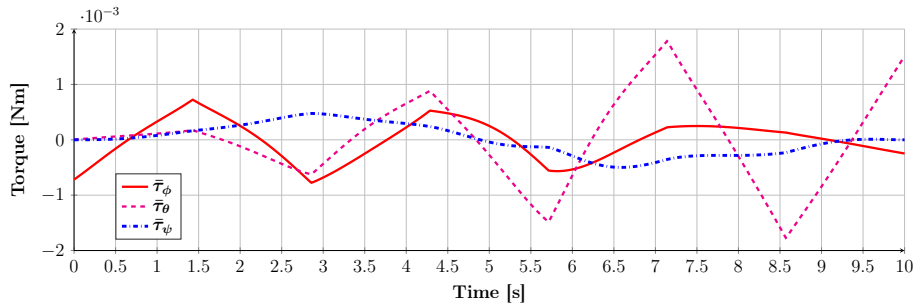
(a) Flat position on the three axes and the control points.



(b) Flat reference angles, roll, pitch and yaw.



(c) Flat reference of the thrust force.



(d) Flat reference of the angle torques.

Figure 4: Flat references for positions, angles, thrust and angle torques.

Control Scheme	K_p	K_d	K_i
Torque controller 4.2 used in 4.4,4.6	$diag\{225, 225, 225\}$	$diag\{30, 30, 30\}$	$diag\{0, 0, 0\}$
Attitude controller 4.3 used in 4.5,4.6	$diag\{25, 25, 9\}$	$diag\{10, 10, 6\}$	$diag\{1, 1, 0.3\}$

Table 1: Parameters of rotation and attitude controller

Controller	IAE	IAE
	no wind	wind gust
Flat angle tracking 4.4	0.0151	52.2087
Flat position tracking 4.5	0.7210	0.9419
Combined flat angle and position tracking 4.6	0.0227	0.6221

Table 2: Integral Absolute magnitude of Errors (IAE) of positions using the control strategies in Section 4.

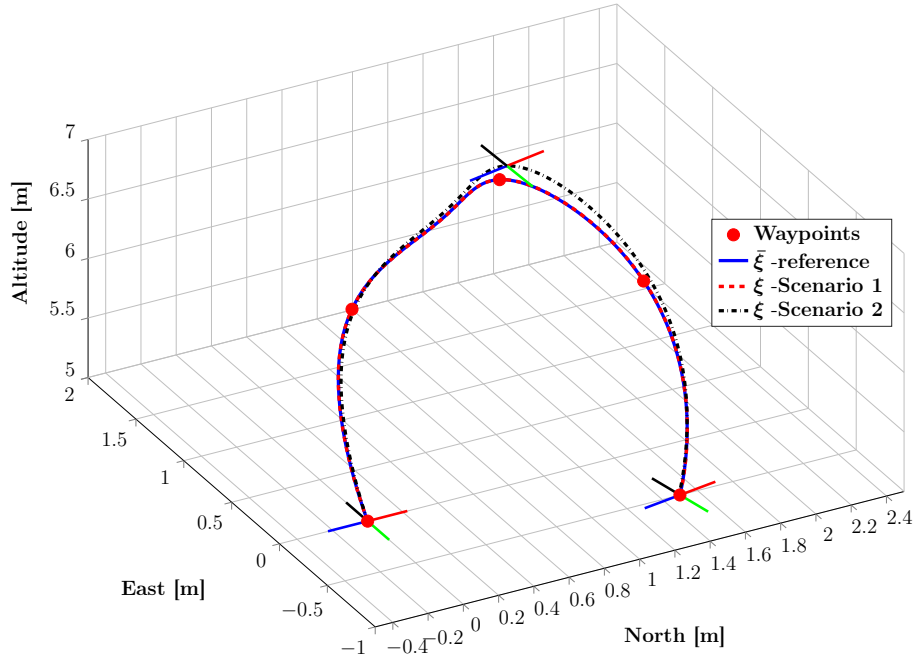


Figure 5: Trajectories of quadcopter under different scenarios.

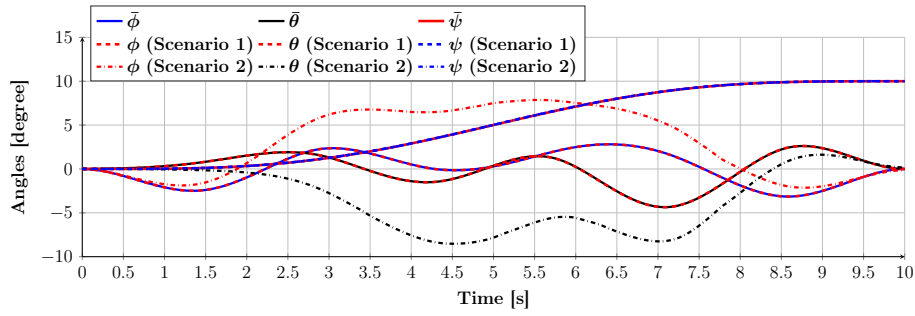


Figure 6: Roll, pitch, yaw angles of quadcopter under different scenarios.

For comparison, in each simulation case we take the Integral of Absolute magnitude of the Error (IAE) over the position: $IAE = \int_{t_0=0}^{t_f=10} \|\bar{\xi} - \xi\| dt$. The results are gathered in Table 2, which leads us to several observations. First of all, under nominal functioning (no wind) the three controllers are comparable,

390 i.e, the IAE values are small and not far away from each other, with controller
4.4 being slightly better. However, in the presence of high disturbances, the
controller 4.4 fails as we also indicated in Section 4.4 (IAE= 52.2087 is too large
comparing to the others). In contrast, the flat position tracking controller 4.5
and the combined flat angle and position tracking controller 4.6 have proven
395 their trajectory tracking capabilities even for high wind conditions. Note that,
the combined flat angle and position tracking controller 4.6 is behaving best,
this being, in our opinion, the most effective control strategy.

We provide illustrations of simulation results for two scenarios:

- Scenario 1: the aim is to track the reference using flat angle tracking
400 controller detailed in Section 4.4 with no wind condition;
- Scenario 2: the aim is to track the reference using combined flat angle
and position tracking controller detailed in Section 4.6 in the wind blow
condition with maximum wind speed up to 25 [km/h];

Figure 5 illustrates the quadcopter actual motions resulted for the two sce-
405 narios (for the scenario 1 the actual trajectory is plotted in solid blue line and
for the scenario 2 in dash-dotted black line) comparing to the reference trajec-
tory given in dash-dotted red line. It can be seen that the differences w.r.t. the
reference are very small although the maximum wind speed of 25 [km/h] is such
a difficult condition for trajectory tracking of small-scale UAV in general.

410 For the scenario 2, Figure 5 and 6 illustrate the quadcopter blown in the
positive directions of the IF (East–North–Up coordinate) due to a wind profile
from north-east. Figure 6 proves the effectiveness of the combined flat angle
and position tracking controller 4.6 which appropriately tilted the quadcopter
to fight against the northeast wind blow.

415 Our simulations have proven that the various control strategies described
in the paper are all capable to track the trajectory in the nominal case and,
with specific degree of accuracy, the flat position tracking controller 4.5 and the
combined flat angle and position tracking controller 4.6 are effective to track
the trajectory in more challenging conditions. The robustness of the controllers

420 can be further enhanced by choosing different corrective terms and/or different
parameters.

5.2. Discussions

Detailed comparisons are difficult to provide since most of the papers treating
this topic provide incomplet data for the flatness generation and inner control
425 loops design makes a point-by-point simulation hard to accomplish, we note,
however, several remarks which prove the novel elements of our flatness-based
control approach with respect to the references [15, 21, 3, 32].

1. The flat trajectories generated are not always used in simulation. For
example, in [3] the reference tracked is actually a sequence of delayed step
430 functions. In our opinion this actually discards the major advantage of
flat parametrizations, that is, of ensuring a feasible trajectory.
2. The flat output parametrizations often use simple representations (mono-
nomials in [15] or cubic splines in [21]). These implementations strongly
limit the number of constraints which can be considered and may lead to
435 numerical issues. In contrast, the b-spline parametrization used in this
paper offers smoothness guarantees, is impervious to the number of con-
straints (in the sense that the degree of the functions does not depend
on them) and, most importantly, offers an analytical framework for cost
minimizations (e.g., for trajectory length).
- 440 3. All flat implementations encountered in the literature consider simplifying
assumptions (yaw angle kept constant, small angles, etc). In contrast, the
flat representation proposed in 28 and presented in Section 3 can provide
explicit (and free of trigonometric terms) descriptions of all state and
input components of the quadcopter dynamics. In particular, the angles
445 and torques have a more compact representation, see Appendix A for
details. While the resulting flat representations (especially for torques)
are still cumbersome, they are nonetheless much more compact than the
representations which assume the standard flat output detailed in Remark
2 (quantitatively, the difference in formulation length is of an order of

450 magnitude). Not in the least, the novel approach proposed here can be
easily employed in similar schemes proposed in the literature [15, 21, 3, 32]
and will lead to simpler formulations and thus to more efficient control
loops.

4. In many cases (and in the strategy proposed in Section 4) the flat angles
455 are used as references for low-level control loops (the ones providing the
angle torque values). Many papers employ PD or similar control schemes
[3, 32] which we consider to be an inferior alternative to the torque control
approach 4.2 proposed here. Assuming accurate parameter measurements
this strategy provides a closed-loop linearized rotation dynamic which can
460 handle abrupt reference changes and has a good tracking performances.

5. An aspect sometimes neglected [15, 21] is the difference between angular
velocities and the Euler angles rates (an acceptable assumption for small
roll and pitch values). While this simplification leads to simpler torque and
angle formulations it becomes imprecise at large roll and pitch values and
465 leads thus to imprecise angle tracking. Therefore, while [15, 21] propose
strategies similar with the flat position tracking from Section 4.5, our
approach can accurately handle the nonlinearities introduced by the Euler
angles and permits to track the position components.

6. Conclusions

470 This paper addressed the challenging trajectory tracking problem for quad-
copter systems using an effective combination between differential flatness and
feedback linearization. Classified as severely underactuated systems, detailed
kinematic and dynamical models of a quadcopter were required. Next, a ref-
erence trajectory was generated off-line using an original flat representation.
475 On-line, feedback linearization-based controllers via flatness were designed for
tracking the feasible reference. The power of flat output characterization allow-
ing full flat parametrization of states and inputs, and the state feedback control
methods applied for the original nonlinear quadcopter dynamics system without

any loss of precision shows promise. These were detailed and validated through
480 proof of concept examples, illustrations and simulation results.

The original contributions stem from:

- the flat trajectory construction for the strongly nonlinear quadcopter system which provided positions, angles, thrust and torques;
- the control strategies based on feedback linearization (i.e., flat angle tracking,
485 flat position tracking) which allowed both orientation and position control without any simplification on the quadcopter system.

Future work will concentrate on the introduction of bounded/stochastic disturbances and trajectory reconfiguration mechanisms.

References

490 References

- [1] W. Dong, G.-Y. Gu, X. Zhu, H. Ding, A high-performance flight control approach for quadrotors using a modified active disturbance rejection technique, *Robotics and Autonomous Systems*.
- [2] C. Ha, Z. Zuo, F. B. Choi, D. Lee, Passivity-based adaptive backstepping
495 control of quadrotor-type uavs, *Robotics and Autonomous Systems* 62 (9) (2014) 1305–1315.
- [3] S. Formentin, M. Lovera, Flatness-based control of a quadrotor helicopter via feedforward linearization., in: *CDC-ECE*, 2011, pp. 6171–6176.
- [4] M. Khan, Quadcopter flight dynamics, *International Journal of Science and
500 Technology Research* (2014) 130–135.
- [5] N. Sydney, B. Smyth, D. A. Paley, Dynamic control of autonomous quadrotor flight in an estimated wind field, in: *Decision and Control (CDC)*, 2013 IEEE 52nd Annual Conference on, IEEE, 2013, pp. 3609–3616.

- [6] I. Sa, P. Corke, Estimation and control for an open-source quadcopter, in: Proceedings of the Australasian Conference on Robotics and Automation 2011, 2011.
- [7] J. G. Leishman, The breguet-richet quad-rotor helicopter of 1907, *Vertiflite*, v. 47, no. 3 (Summer 2001), p. 58-60: ill.
- [8] A. Chovancová, T. Fico, P. Hubinský, F. Duchoň, Comparison of various quaternion-based control methods applied to quadrotor with disturbance observer and position estimator, *Robotics and Autonomous Systems* 79 (2016) 87–98.
- [9] S. Markman, B. Holder, Bell/boeing v-22 osprey tilt-engine vtol transport (usa), *Straight Up: A History of Vertical Flight*.
- [10] Phantom 4 (2016).
URL <https://www.dji.com/>
- [11] Medical Ambulance Drone (2015).
URL <https://www.argodesign.com/>
- [12] I. Prodan, S. Olaru, R. Bencatel, J. Sousa, C. Stoica, S. Niculescu, Receding horizon flight control for trajectory tracking of autonomous aerial vehicles, *Control Engineering Practice* 21 (10) (2013) 1334–1349. doi:10.1016/j.conengprac.2013.05.010.
- [13] M. Fliess, J. Lévine, P. Martin, P. Rouchon, Flatness and defect of non-linear systems: introductory theory and examples, *International journal of control* 61 (6) (1995) 1327–1361.
- [14] K. Sreenath, T. Lee, V. Kumar, Geometric control and differential flatness of a quadrotor uav with a cable-suspended load, in: Proceedings of the 52nd IEEE Conference on Conference on Decision and Control, IEEE, 2013, pp. 2269–2274.

- 530 [15] A. Chamseddine, Y. Zhang, C. Rabbath, C. Join, D. Theilliol, Flatness-based trajectory planning/replanning for a quadrotor unmanned aerial vehicle, *IEEE Transactions on Aerospace and Electronic Systems* 48 (4) (2012) 2832–2848.
- [16] K. Sreenath, V. Kumar, Dynamics, control and planning for cooperative
535 manipulation of payloads suspended by cables from multiple quadrotor robots, *Robotics: Science and Systems* 1 (2013) 81–116.
- [17] S. Bouabdallah, P. Murrieri, R. Siegwart, Design and control of an indoor micro quadrotor, in: *Robotics and Automation, 2004. Proceedings. ICRA'04. 2004 IEEE International Conference on*, Vol. 5, IEEE, pp. 4393–
540 4398.
- [18] L. M. Argentim, W. C. Rezende, P. E. Santos, R. A. Aguiar, Pid, lqr and lqr-pid on a quadcopter platform, in: *Informatics, Electronics & Vision (ICIEV), 2013 International Conference on*, IEEE, 2013, pp. 1–6.
- [19] V. Kodgirwar, V. Kumar, S. Sawant, M. Shegokar, Design of control system
545 for quadcopter using complementary filter and pid controller, in: *International Journal of Engineering Research and Technology*, Vol. 3, ESRSA Publications, 2014.
- [20] S. G. Tzafestas, *Introduction to mobile robot control*, Elsevier, 2013.
- [21] G. Rivera, O. Sawodny, Flatness-based tracking control and nonlinear observer
550 for a micro aerial quadcopter, in: *ICNAAM 2010: International Conference of Numerical Analysis and Applied Mathematics 2010*, Vol. 1281, AIP Publishing, 2010, pp. 386–389.
- [22] F. Stoican, I. Prodan, D. Popescu, Flat trajectory generation for waypoints relaxations and obstacle avoidance, in: *Proceedings of the 23th IEEE Mediterranean Conference on Control and Automation*, IEEE, 2015, pp.
555 695–700.

- [23] R. W. Fox, A. T. McDonald, Introduction to fluid mechanics, John Wiley, 1994.
- [24] J. Lévine, On necessary and sufficient conditions for differential flatness, *Applicable Algebra in Engineering, Communication and Computing* 22 (1) (2011) 47–90.
- [25] J. Wilkinson, The algebraic eigenvalue problem, Vol. 155, Oxford Univ. Press, 1965.
- [26] F. Suryawan, Constrained trajectory generation and fault tolerant control based on differential flatness and b-splines, Ph.D. thesis, School of Electrical Engineering and Computer Science, The University of Newcastle, Australia (2012).
- [27] J. De Doná, F. Suryawan, M. Seron, J. Lévine, A flatness-based iterative method for reference trajectory generation in constrained NMPC, *Int. Workshop on Assessment and Future Direction of Nonlinear Model Predictive Control* (2009) 325–333.
- [28] L. Piegl, W. Tiller, B-spline curves and surfaces, in: *The NURBS Book*, Springer, 1995, pp. 81–116.
- [29] K. Bipin, V. Duggal, K. M. Krishna, Autonomous navigation of generic quadcopter with minimum time trajectory planning and control, in: *Vehicular Electronics and Safety (ICVES), 2014 IEEE International Conference on*, IEEE, 2014, pp. 66–71.
- [30] J. J. Craig, Introduction to robotics: mechanics and control, Vol. 3, Pearson Prentice Hall Upper Saddle River, 2005.
- [31] J. Jang, H. Gong, J. Lyou, Computed torque control of an aerospace craft using nonlinear inverse model and rotation matrix, in: *Proceedings of the 15th International Conference on Control, Automation and Systems*, IEEE, 2015, pp. 1743–1746.

- [32] D. Mellinger, V. Kumar, Minimum snap trajectory generation and control
585 for quadrotors, in: Robotics and Automation (ICRA), 2011 IEEE International Conference on, IEEE, 2011, pp. 2520–2525.
- [33] Crazyflie 2.0 (2015).
URL <https://www.bitcraze.io/>
- [34] J. Löfberg, Yalmip : A toolbox for modeling and optimization in MATLAB,
590 in: Proceedings of the CACSD Conference, Taipei, Taiwan, 2004.
URL <http://users.isy.liu.se/johanl/yalmip>
- [35] M. Herceg, M. Kvasnica, C. Jones, M. Morari, Multi-Parametric Toolbox 3.0, in: Proc. of the European Control Conference, Zürich, Switzerland, 2013, pp. 502–510, <http://control.ee.ethz.ch/~mpt>.

595 **Appendix A. Flat representation (29)–(33) for the quadcopter dynamics (26)–(27)**

Appendix A.1. Position, angle and thrust components of the quadcopter dynamics (26)–(27)

Position components expressed in term of the flat output:

$$x = z_1, \quad (\text{A.1a})$$

$$y = z_2, \quad (\text{A.1b})$$

$$z = z_3. \quad (\text{A.1c})$$

Angle components expressed in term of the flat output:

$$\phi = \arcsin \left(\frac{2z_4\ddot{z}_1 - (1 - z_4^2)\ddot{z}_2}{(1 + z_4^2)\sqrt{\ddot{z}_1^2 + \ddot{z}_2^2 + (\ddot{z}_3 + g)^2}} \right), \quad (\text{A.2a})$$

$$\theta = \arctan \left(\frac{(1 - z_4^2)\ddot{z}_1 + 2z_4\ddot{z}_2}{(1 + z_4^2)(\ddot{z}_3 + g)} \right), \quad (\text{A.2b})$$

$$\psi = 2 \arctan(z_4). \quad (\text{A.2c})$$

Thrust expressed in term of the flat output:

$$T = m\sqrt{\ddot{z}_1^2 + \ddot{z}_2^2 + (\ddot{z}_3 + g)^2}. \quad (\text{A.3})$$

Torques expressed in term of $[k_1, k_2, k_3, z_4] = [\ddot{z}_1, \ddot{z}_2, \ddot{z}_3, z_4]$:

$$\begin{aligned}
\tau_\phi = I_{xx} & \left(\frac{1}{\sqrt{1 - \frac{(2z_4 k_1 - (1 - z_4^2) k_2)^2}{(1 + z_4^2)^2 (k_1^2 + k_2^2 + k_3^2)}}} \left(\frac{1}{(1 + z_4^2) \sqrt{k_1^2 + k_2^2 + k_3^2}} \left(2\ddot{z}_4 k_1 \right. \right. \right. \\
& + 4\dot{z}_4 \dot{k}_1 + 2z_4 \ddot{k}_1 + 2\ddot{z}_4^2 k_2 + 2z_4 \ddot{z}_4 k_2 + 4z_4 \dot{z}_4 \dot{k}_2 - (1 - z_4^2) \ddot{k}_2 \Big) \\
& - \frac{4 \left(2\ddot{z}_4 k_1 + 2z_4 \dot{k}_1 + 2z_4 \dot{z}_4 k_2 - (1 - z_4^2) \dot{k}_2 \right) z_4 \dot{z}_4}{(1 + z_4^2)^2 \sqrt{k_1^2 + k_2^2 + k_3^2}} + \frac{8 \left(2z_4 k_1 - (1 - z_4^2) k_2 \right) z_4^2 \dot{z}_4^2}{(1 + z_4^2)^3 \sqrt{k_1^2 + k_2^2 + k_3^2}} \\
& - \frac{2 \left(2z_4 k_1 - (1 - z_4^2) k_2 \right) \dot{z}_4^2 + 2 \left(2z_4 k_1 - (1 - z_4^2) k_2 \right) z_4 \ddot{z}_4}{(1 + z_4^2)^2 \sqrt{k_1^2 + k_2^2 + k_3^2}} \\
& - \frac{\left(2\dot{z}_4 k_1 + 2z_4 \dot{k}_1 + 2z_4 \dot{z}_4 k_2 - (1 - z_4^2) \dot{k}_2 \right) \left(2k_1 \dot{k}_1 + 2k_2 \dot{k}_2 + 2k_3 \dot{k}_3 \right)}{(1 + z_4^2) (k_1^2 + k_2^2 + k_3^2)^{3/2}} \\
& - \frac{\left(2z_4 k_1 - (1 - z_4^2) k_2 \right) \left(\dot{k}_1^2 + k_1 \ddot{k}_1 + \dot{k}_2^2 + k_2 \ddot{k}_2 + \dot{k}_3^2 + k_3 \ddot{k}_3 \right)}{(1 + z_4^2) (k_1^2 + k_2^2 + k_3^2)^{3/2}} \\
& + \frac{2 \left(2z_4 k_1 - (1 - z_4^2) k_2 \right) \left(2k_1 \dot{k}_1 + 2k_2 \dot{k}_2 + 2k_3 \dot{k}_3 \right) z_4 \dot{z}_4}{(1 + z_4^2)^2 (k_1^2 + k_2^2 + k_3^2)^{3/2}} \\
& + \frac{3 \left(2z_4 k_1 - (1 - z_4^2) k_2 \right) \left(k_1 \dot{k}_1 + k_2 \dot{k}_2 + k_3 \dot{k}_3 \right)^2}{(1 + z_4^2) (k_1^2 + k_2^2 + k_3^2)^{5/2}} \Big) \\
& - \frac{1}{2} \frac{1}{\left(1 - \frac{(2z_4 k_1 - (1 - z_4^2) k_2)^2}{(1 + z_4^2)^2 (k_1^2 + k_2^2 + k_3^2)} \right)^{3/2}} \left(\frac{2\dot{z}_4 k_1 + 2z_4 \dot{k}_1 + 2z_4 \dot{z}_4 k_2 - (1 - z_4^2) \dot{k}_2}{(1 + z_4^2) \sqrt{k_1^2 + k_2^2 + k_3^2}} \right. \\
& \left. - \frac{2 \left(2z_4 k_1 - (1 - z_4^2) k_2 \right) z_4 \dot{z}_4}{(1 + z_4^2)^2 \sqrt{k_1^2 + k_2^2 + k_3^2}} - \frac{\left(2z_4 k_1 - (1 - z_4^2) k_2 \right) \left(k_1 \dot{k}_1 + k_2 \dot{k}_2 + k_3 \dot{k}_3 \right)}{(1 + z_4^2) (k_1^2 + k_2^2 + k_3^2)^{3/2}} \right) \\
& \left(\frac{2 \left(2z_4 k_1 - (1 - z_4^2) k_2 \right) \left(2\dot{z}_4 k_1 + 2z_4 \dot{k}_1 + 2z_4 \dot{z}_4 k_2 - (1 - z_4^2) \dot{k}_2 \right)}{(1 + z_4^2)^2 (k_1^2 + k_2^2 + k_3^2)} \right. \\
& \left. + \frac{4 \left(2z_4 k_1 - (1 - z_4^2) k_2 \right)^2 z_4 \dot{z}_4}{(1 + z_4^2)^3 (k_1^2 + k_2^2 + k_3^2)} + \frac{\left(2z_4 k_1 - (1 - z_4^2) k_2 \right)^2 \left(2k_1 \dot{k}_1 + 2k_2 \dot{k}_2 + 2k_3 \dot{k}_3 \right)}{(1 + z_4^2)^2 (k_1^2 + k_2^2 + k_3^2)^2} \right) \\
& - \frac{2 \left(-2z_4 \dot{z}_4 k_1 + (1 - z_4^2) \dot{k}_1 + 2\dot{z}_4 k_2 + 2z_4 \dot{k}_2 \right) \dot{z}_4}{k_3 (1 + z_4^2)^2 \sqrt{1 + \frac{\left((1 - z_4^2) k_1 + 2z_4 k_2 \right)^2}{k_3^2 (1 + z_4^2)^2}}} + \frac{2 \left((1 - z_4^2) k_1 + 2z_4 k_2 \right) \dot{z}_4 \dot{k}_3}{k_3^2 (1 + z_4^2)^2 \sqrt{1 + \frac{\left((1 - z_4^2) k_1 + 2z_4 k_2 \right)^2}{k_3^2 (1 + z_4^2)^2}}}
\end{aligned}$$

$$\begin{aligned}
\tau_\theta = I_{yy} & \left(\frac{1}{2} \left(\left(\frac{-2z_4\dot{z}_4k_1 + (1-z_4^2)\dot{k}_1 + 2\dot{z}_4k_2 + 2z_4\dot{k}_2}{k_3(1+z_4^2)} - \frac{((1-z_4^2)k_1 + 2z_4k_2)\dot{k}_3}{k_3^2(1+z_4^2)} \right. \right. \right. \\
& - \frac{2z_4\dot{z}_4((1-z_4^2)k_1 + 2z_4k_2)}{k_3(1+z_4^2)^2} \left. \left. \left(-\frac{2(2z_4k_1 - (1-z_4^2)k_2)(2\dot{z}_4k_1 + 2z_4\dot{k}_1 + 2z_4\dot{z}_4k_2 - (1-z_4^2)\dot{k}_2)}{(1+z_4^2)^2(k_1^2 + k_2^2 + k_3^2)} \right. \right. \right. \\
& + \frac{4z_4\dot{z}_4(2z_4k_1 - (1-z_4^2)k_2)^2}{(1+z_4^2)^3(k_1^2 + k_2^2 + k_3^2)} + \frac{2k_1\dot{k}_1(2z_4k_1 - (1-z_4^2)k_2)^2 + 2k_2\dot{k}_2 + 2k_3\dot{k}_3}{(1+z_4^2)^2(k_1^2 + k_2^2 + k_3^2)^2} \left. \left. \right) \right) / \\
& \left(\sqrt{1 - \frac{(2z_4k_1 - (1-z_4^2)k_2)^2}{(1+z_4^2)^2(k_1^2 + k_2^2 + k_3^2)}} \left(1 + \frac{((1-z_4^2)k_1 + 2z_4k_2)^2}{k_3^2(1+z_4^2)^2} \right) + \frac{1}{1 + \frac{((1-z_4^2)k_1 + 2z_4k_2)^2}{k_3^2(1+z_4^2)^2}} \right) \\
& \sqrt{1 - \frac{(2z_4k_1 - (1-z_4^2)k_2)^2}{(1+z_4^2)^2(k_1^2 + k_2^2 + k_3^2)}} \left(\frac{4((1-z_4^2)k_1 + 2z_4k_2)\dot{k}_3z_4\dot{z}_4 - ((1-z_4^2)k_1 + 2z_4k_2)\dot{k}_3^2}{k_3^2(1+z_4^2)^2} \right. \\
& + \frac{-2\dot{z}_4^2k_1 - 2z_4\dot{z}_4\dot{k}_1 - 4z_4\dot{z}_4\dot{z}_1 + (1-z_4^2)\ddot{k}_1 + 2\dot{z}_4\dot{k}_2 + 4\dot{z}_4\dot{k}_2 + 2z_4\ddot{k}_2}{k_3(1+z_4^2)} + \frac{8((1-z_4^2)k_1 + 2z_4k_2)z_4^2\dot{z}_4^2}{k_3(1+z_4^2)^3} \\
& - \frac{2\dot{k}_3(-2z_4\dot{z}_4k_1 + (1-z_4^2)\dot{k}_1 + 2\dot{z}_4k_2 + 2z_4\dot{k}_2)}{k_3^2(1+z_4^2)} + \frac{2((1-z_4^2)k_1 + 2z_4k_2)\dot{k}_3^2}{k_3^3(1+z_4^2)} \\
& \left. - \frac{4(-2z_4\dot{z}_4k_1 + (1-z_4^2)\dot{k}_1 + 2\dot{z}_4k_2 + 2z_4\dot{k}_2)z_4\dot{z}_4 + 2((1-z_4^2)k_1 + 2z_4k_2)(\dot{z}_4^2 + z_4\dot{z}_4)}{k_3(1+z_4^2)^2} \right) \\
& - \frac{1}{\left(1 + \frac{(1-z_4^2)k_1 + 2z_4k_2}{k_3^2(1+z_4^2)^2} \right)^2} \left(\sqrt{1 - \frac{(2z_4k_1 - (1-z_4^2)k_2)^2}{(1+z_4^2)^2(k_1^2 + k_2^2 + k_3^2)}} \left(-\frac{((1-z_4^2)k_1 + 2z_4k_2)\dot{k}_3}{k_3^2(1+z_4^2)} \right. \right. \\
& + \frac{-2z_4\dot{z}_4k_1 + (1-z_4^2)\dot{k}_1 + 2\dot{z}_4k_2 + 2z_4\dot{k}_2}{k_3(1+z_4^2)} - \frac{2((1-z_4^2)k_1 + 2z_4k_2)z_4\dot{z}_4}{k_3(1+z_4^2)^2} \left. \right) \\
& \left(\frac{2((1-z_4^2)k_1 + 2z_4k_2)(-2z_4\dot{z}_4k_1 + (1-z_4^2)\dot{k}_1 + 2\dot{z}_4k_2 + 2z_4\dot{k}_2)}{k_3^2(1+z_4^2)^2} - \frac{2(1-z_4^2)k_1 + 2z_4k_2}{k_3^3(1+z_4^2)^2} \right. \\
& \left. - \frac{4((1-z_4^2)k_1 + 2z_4k_2)^2z_4\dot{z}_4}{k_3^2(1+z_4^2)^3} \right) + \frac{2(2\dot{z}_4k_1 + 2z_4\dot{k}_1 + 2z_4\dot{z}_4k_2 - (1-z_4^2)\dot{k}_2)\dot{z}_4}{(1+z_4^2)^2\sqrt{k_1^2 + k_2^2 + k_3^2}\sqrt{1 + \frac{((1-z_4^2)k_1 + 2z_4k_2)^2}{k_3^2(1+z_4^2)^2}}} \\
& - \frac{8(2z_4k_1 - (1-z_4^2)k_2)\dot{z}_4^2z_4}{(1+z_4^2)^3\sqrt{k_1^2 + k_2^2 + k_3^2}\sqrt{1 + \frac{((1-z_4^2)k_1 + 2z_4k_2)^2}{k_3^2(1+z_4^2)^2}}}
\end{aligned}$$

$$\begin{aligned}
& - \frac{z_4 (2z_4 k_1 - (1 - z_4^2) k_2) (2k_1 \dot{k}_1 + 2k_2 \dot{k}_2 + 2k_3 \dot{k}_3)}{(1 + z_4^2)^2 (k_1^2 + k_2^2 + k_3^2)^{3/2} \sqrt{1 + \frac{((1 - z_4^2) k_1 + 2z_4 k_2)^2}{k_3^2 (1 + z_4^2)^2}}} \\
& - \frac{1}{(1 + z_4^2)^2 (k_1^2 + k_2^2 + k_3^2)^{3/2} \left(1 + \frac{((1 - z_4^2) k_1 + 2z_4 k_2)^2}{k_3^2 (1 + z_4^2)^2}\right)^{3/2}} \left((2z_4 k_1 - (1 - z_4^2) k_2) \dot{z}_4 \right. \\
& \left. \left(\frac{2((1 - z_4^2) k_1 + 2z_4 k_2) (-2z_4 \dot{z}_4 k_1 + (1 - z_4^2) \dot{k}_1 + 2z_4 \dot{k}_2 + 2z_4 \dot{k}_3)}{k_3^2 (1 + z_4^2)^2} - \frac{2((1 - z_4^2) k_1 + 2z_4 k_2)^2 \dot{k}_3}{k_3^2 (1 + z_4^2)^2} \right. \right. \\
& \left. \left. - \frac{4((1 - z_4^2) k_1 + 2z_4 k_2)^2 z_4 \dot{z}_4}{k_3^2 (1 + z_4^2)^3} \right) + \frac{2(2z_4 k_1 - (1 - z_4^2) k_2) \ddot{z}_4}{(1 + z_4^2)^2 (k_1^2 + k_2^2 + k_3^2)^{3/2} \sqrt{1 + \frac{((1 - z_4^2) k_1 + 2z_4 k_2)^2}{k_3^2 (1 + z_4^2)^2}}} \right) \\
& - (I_{zz} - I_{xx}) \left(\frac{1}{\sqrt{1 - \frac{(2z_4 k_1 - (1 - z_4^2) k_2)^2}{(1 + z_4^2)^2 (k_1^2 + k_2^2 + k_3^2)}}} \left(\frac{2z_4 \dot{z}_4 k_1 + 2z_4 \dot{k}_1 + 2z_4 \dot{z}_4 k_2 - (1 - z_4^2) \dot{k}_2}{(1 + z_4^2) \sqrt{k_1^2 + k_2^2 + k_3^2}} \right. \right. \\
& \left. \left. - \frac{2(2z_4 k_1 - (1 - z_4^2) k_2) z_4 \dot{z}_4}{(1 + z_4^2)^2 \sqrt{k_1^2 + k_2^2 + k_3^2}} - \frac{(2z_4 k_1 - (1 - z_4^2) k_2) (k_1 \dot{k}_1 + k_2 \dot{k}_2 + k_3 \dot{k}_3)}{(1 + z_4^2) (k_1^2 + k_2^2 + k_3^2)^{3/2}} \right) \right. \\
& \left. - \frac{2((1 - z_4^2) k_1 + 2z_4 k_2) \dot{z}_4}{k_3 (1 + z_4^2)^2 \sqrt{1 + \frac{((1 - z_4^2) k_1 + 2z_4 k_2)^2}{k_3^2 (1 + z_4^2)^2}}} \left(- \frac{1}{(1 + z_4^2)^2 \sqrt{k_1^2 + k_2^2 + k_3^2}} \left(1 + \frac{((1 - z_4^2) k_1 + 2z_4 k_2)^2}{k_3^2 (1 + z_4^2)^2} \right) \right) \right) \\
& (2z_4 k_1 - (1 - z_4^2) k_2) \left(\frac{-2z_4 \dot{z}_4 k_1 + (1 - z_4^2) \dot{k}_1 + 2z_4 \dot{k}_2 + 2z_4 \dot{k}_3}{k_3 (1 + z_4^2)} - \frac{((1 - z_4^2) k_1 + 2z_4 k_2) \dot{k}_3}{k_3^2 (1 + z_4^2)} \right. \\
& \left. - \frac{2((1 - z_4^2) k_1 + 2z_4 k_2) z_4 \dot{z}_4}{k_3 (1 + z_4^2)^2} \right) + \frac{2z_4 \sqrt{1 - \frac{(2z_4 k_1 - (1 - z_4^2) k_2)^2}{(1 + z_4^2)^2 (k_1^2 + k_2^2 + k_3^2)}}}{(1 + z_4^2) \sqrt{1 + \frac{((1 - z_4^2) k_1 + 2z_4 k_2)^2}{k_3^2 (1 + z_4^2)^2}}}
\end{aligned} \tag{A.5}$$

$$\begin{aligned}
\tau_\psi = I_{zz} & \left(- \frac{1}{(1+z_4^2)^2 \sqrt{k_1^2+k_2^2+k_3^2} \left(1 + \frac{\left((1-z_4^2)k_1+2z_4k_2 \right)^2}{k_3^2(1+z_4^2)^2} \right)} \left((2\dot{z}_4k_1+2z_4\dot{k}_1+2z_4\dot{z}_4k_2 \right. \right. \\
& - (1-z_4^2)\dot{k}_2 \left. \left(\frac{-2z_4\dot{z}_4k_1+(1-z_4^2)\dot{k}_1+2\dot{z}_4k_2+2z_4\dot{k}_2}{k_3(1+z_4^2)} - \frac{\left((1-z_4^2)k_1+2z_4k_2 \right) \dot{k}_3}{k_3^2(1+z_4^2)} \right. \right. \\
& \left. \left. - \frac{2\left((1-z_4^2)k_1+2z_4k_2 \right) z_4\dot{z}_4}{k_3(1+z_4^2)^2} \right) z_4\dot{z}_4 \right) + \frac{1}{2} \frac{1}{(1+z_4^2)^2(k_1^2+k_2^2+k_3^2)^{3/2} \left(1 + \frac{\left((1-z_4^2)k_1+2z_4k_2 \right)^2}{k_3^2(1+z_4^2)^2} \right)} \\
& \left((2z_4k_1-(1-z_4^2)k_2) \left(\frac{-2z_4\dot{z}_4k_1+(1-z_4^2)\dot{k}_1+2\dot{z}_4k_2+2z_4\dot{k}_2}{k_3(1+z_4^2)} - \frac{\left((1-z_4^2)k_1+2z_4k_2 \right) \dot{k}_3}{k_3^2(1+z_4^2)} \right. \right. \\
& \left. \left. - \frac{2\left((1-z_4^2)k_1+2z_4k_2 \right) z_4\dot{z}_4}{k_3(1+z_4^2)^2} \right) (2k_1\dot{k}_1+2k_2\dot{k}_2+2k_3\dot{k}_3) \right) \\
& - \frac{1}{(1+z_4^2)\sqrt{k_1^2+k_2^2+k_3^2} \left(1 + \frac{\left((1-z_4^2)k_1+2z_4k_2 \right)^2}{k_3^2(1+z_4^2)^2} \right)} \left((2z_4k_1-(1-z_4^2)k_2) \left(\frac{1}{k_3(1+z_4^2)} \left(\right. \right. \right. \\
& \left. \left. - 2\dot{z}_4^2k_1-2z_4\dot{z}_4k_1-4z_4\dot{z}_4\dot{k}_1+(1-z_4^2)\ddot{k}_1+2\ddot{z}_4k_2+4\dot{z}_4\dot{k}_2+2z_4\ddot{k}_2 \right) \right. \\
& \left. \left. - \frac{2\left(-2z_4\dot{z}_4k_1+(1-z_4^2)\dot{k}_1+2\dot{z}_4k_2+2z_4\dot{k}_2 \right) \dot{k}_3}{k_3^2(1+z_4^2)} - \frac{4\left(-2z_4\dot{z}_4k_1+(1-z_4^2)\dot{k}_1+2\dot{z}_4k_2+2z_4\dot{k}_2 \right) z_4\dot{z}_4}{k_3(1+z_4^2)^2} \right. \right. \\
& \left. \left. + \frac{2\left((1-z_4^2)k_1+2z_4k_2 \right) \dot{k}_3^2}{k_3^3(1+z_4^2)} + \frac{4\left((1-z_4^2)k_1+2z_4k_2 \right) \dot{k}_3z_4\dot{z}_4}{k_3^2(1+z_4^2)^2} - \frac{\left((1-z_4^2)k_1+2z_4k_2 \right) \ddot{k}_3}{k_3^2(1+z_4^2)} \right. \right. \\
& \left. \left. + \frac{8\left((1-z_4^2)k_1+2z_4k_2 \right) z_4^2\dot{z}_4^2}{k_3(1+z_4^2)^3} - \frac{2\left((1-z_4^2)k_1+2z_4k_2 \right) (z_4^2+z_4\dot{z}_4)}{k_3(1+z_4^2)^2} \right) \right) \\
& + \frac{1}{(1+z_4^2)\sqrt{k_1^2+k_2^2+k_3^2} \left(1 + \frac{\left((1-z_4^2)k_1+2z_4k_2 \right)^2}{k_3^2(1+z_4^2)^2} \right)^2} \left((2z_4k_1-(1-z_4^2)k_2) \right. \\
& \left(\frac{-2z_4\dot{z}_4k_1+(1-z_4^2)\dot{k}_1+2\dot{z}_4k_2+2z_4\dot{k}_2}{k_3(1+z_4^2)} - \frac{\left((1-z_4^2)k_1+2z_4k_2 \right) \dot{k}_3}{k_3^2(1+z_4^2)} - \frac{2\left((1-z_4^2)k_1+2z_4k_2 \right) z_4\dot{z}_4}{k_3(1+z_4^2)^2} \right. \\
& \left. \left(\frac{2\left((1-z_4^2)k_1+2z_4k_2 \right) \left(-2z_4\dot{z}_4k_1+(1-z_4^2)\dot{k}_1+2\dot{z}_4k_2+2z_4\dot{k}_2 \right)}{k_3^2(1+z_4^2)^2} - \frac{2\left((1-z_4^2)k_1+2z_4k_2 \right)^2 \dot{k}_3}{k_3^3(1+z_4^2)^2} \right. \right. \\
& \left. \left. - \frac{4\left((1-z_4^2)k_1+2z_4k_2 \right)^2 z+4\dot{z}_4}{k_3^2(1+z_4^2)^3} \right) \right) + \left(\dot{z}_4 \left(- \frac{2(2z_4k_1-(1-z_4^2)k_2)(2\dot{z}_4k_1+2z_4\dot{k}_1+2z_4\dot{z}_4k_2-(1-z_4^2)\dot{k}_2)}{(1+z_4^2)^2(k_1^2+k_2^2+k_3^2)} \right) \right)
\end{aligned}$$

$$\begin{aligned}
& + \frac{4(2z_4k_1 - (1 - z_4^2)k_2)^2 z_4 z_4}{(1 + z_4^2)^3 (k_1^2 + k_2^2 + k_3^2)} + \frac{(2z_4k_1 - (1 - z_4^2)k_2)^2 (2k_1 k_1 + 2k_2 k_2 + 2k_3 k_3)}{(1 + z_4^2)^2 (k_1^2 + k_2^2 + k_3^2)^2} \Big) \Big) / \\
& \left(\sqrt{1 - \frac{(2z_4k_1 - (1 - z_4^2)k_2)^2}{(1 + z_4^2)^2 (k_1^2 + k_2^2 + k_3^2)}} \sqrt{1 + \frac{((1 - z_4^2)k_1 + 2z_4k_2)^2}{k_3^2 (1 + z_4^2)^2}} (1 + z_4^2)} \right) \\
& - \frac{1}{\left(1 + \frac{((1 - z_4^2)k_1 + 2z_4k_2)^2}{k_3^2 (1 + z_4^2)^2}\right)^{3/2}} \left(z_4 \sqrt{1 - \frac{(2z_4k_1 - (1 - z_4^2)k_2)^2}{(1 + z_4^2)^2 (k_1^2 + k_2^2 + k_3^2)}} \right. \\
& \left. \frac{2((1 - z_4^2)k_1 + 2z_4k_2) \left(-2z_4 z_4 k_1 + (1 - z_4^2)k_1 + 2z_4k_2 + 2z_4k_2\right)}{k_3^2 (1 + z_4^2)^2} \right) \\
& - \frac{2((1 - z_4^2)k_1 + 2z_4k_2)^2 k_3}{k_3^3 (1 + z_4^2)^2} - \frac{4((1 - z_4^2)k_1 + 2z_4k_2) z_4 z_4}{k_3^2 (1 + z_4^2)^3} \Big) + \frac{2z_4 \sqrt{1 - \frac{(2z_4k_1 - (1 - z_4^2)k_2)^2}{(1 + z_4^2)^2 (k_1^2 + k_2^2 + k_3^2)}}}{(1 + z_4^2) \sqrt{1 + \frac{((1 - z_4^2)k_1 + 2z_4k_2)^2}{k_3^2 (1 + z_4^2)^2}}} \\
& - \frac{4z_4^2 z_4 \sqrt{1 - \frac{(2z_4k_1 - (1 - z_4^2)k_2)^2}{(1 + z_4^2)^2 (k_1^2 + k_2^2 + k_3^2)}}}{(1 + z_4^2)^2 \sqrt{1 + \frac{((1 - z_4^2)k_1 + 2z_4k_2)^2}{k_3^2 (1 + z_4^2)^2}}}
\end{aligned}$$

(A.6)